Amin Modabberian*, Hoang Khac Nguyen, and Kai Zenger

Mean Value Modeling of Maritime Diesel Engines

Abstract: This work aims to develop a first principles mean value model that can be further used for advanced control design on different types of maritime diesel engines to increase efficiency and reduce fuel consumption. A nonlinear model is initially derived and linearised for a control design. These models are simulated and results are compared for further control design approaches.

Keywords: diesel engines, modeling, mean value modeling

***Corresponding Author: Amin Modabberian:** Aalto University, E-mail: amin.modabberian@aalto.fi
Hoang Khac Nguyen: Aalto University, E-mail: hoang.kh.nguyen@aalto.fi
Kai Zenger: Aalto University, Email: kai.zenger@aalto.fi

1 Introduction

As the European emission standards have become more stringent, diesel engines are becoming obsolete especially within the automotive industry [1]. However, diesel engines will be used in maritime transportation for the upcoming decades. Emission minimization of NO_x, CO_2 and particulate matter is one of the major areas in maritime diesel engine control applications. Adhering to emission conditions set by International Maritime Organization (IMO) [2], current diesel engines requires efficient control, which itself require accurate modeling. In this work, a first principles mean value model for diesel engine airpath and engine dynamics are presented, that is, creating a nonlinear and linear models to examine the state variables of the system, which are intake and exhaust manifold pressures, compressor power and engine speed. The airpath model consists of intake and exhaust manifold pressures, turbocharger power, engine speed and fuel injection ratio. Each dynamics is modeled and simulated separately utilizing MATLAB's Simulink. Some of the models are achieved empirically due the nonlinearity of system. On the other hand, such nonlinear models are required for mapping complex chemical and combustion reactions. Mean value model itself is a valid approach. However, it is not suitable for cylinder wise control, since it does not take the pulsating nature of the engine airpath in to account [3][4].

In general, modeling does not possess a single way approach for all dynamic systems. However, numerous valid and widely used approaches exist in the literature[5–9]. Each system and its features, such as physical quantities mentioned above, requires a careful and a systematic approach, which affects the control design and behavior of controls. In other words, the desired efficiency in control design of the engine is highly dependent on the generated mathematical models of the system. Mean value models are also part of the more accurate models to be developed for cylinder-wise control of the engine, which is a key challenge nowadays and in the years to come [10].

The developed mean value model is presented in section 2. Control design and simulation results are presented in sections 3 and 4, respectively.

2 Modelling

The mathematical model in this work is based on the VEBIC's engine provided by Wärtsilä [11]. The topology is depicted in Figure 1. The engine airpath is con-

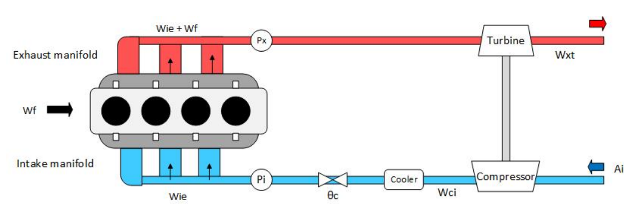

Fig. 1. Topology of the diesel engine

trolled by turbocharger, which consists of turbine and compressor. The compressor increases the incoming air pressure to a desired level in addition to increasing the temperature levels. The air temperature is then decreased with inter-cooler to best suit the combustion reaction. The amount of air mass in the cylinders depends on the fuel injection. Therefore, the intake manifold pressure has to be controlled.

The injected fuel is mixed with heated air mass in cylinder and ignited with a spark. This reaction pushes the piston down. The piston is attached to the crankshaft. Hence, the lateral motion of the piston is converted to rotational motion of the crankshaft. The piston pushes the exhaust gas out of the cylinder toward the turbine. The exhaust gas causes the turbine blades to spin. Since the turbine is attached to the compressor with a shaft, it is possible to control the turbine with the compressor or the intake manifold pressure with turbine speed.[12]

2.1 Airpath model

Mass flows
The conversation of air mass is equal to mass flows through the intake and exhaust manifold [13]. The air mass flow through intake manifold is the difference between the air mass flows into the compressor, W_{ci} $(Kg \cdot s^{-1})$, and cylinders, W_{ie}

$$\dot{m}_i = W_{ci} - W_{ie} \tag{1}$$

The air mass flow though the exhaust manifold is the difference between exhaust mass flow into the turbine, W_{xt}, and sum of air mass flow into the cylinders with fuel mass flow into the cylinders, W_f,

$$\dot{m}_x = W_{ie} + W_f - W_{xt} \tag{2}$$

Manifold pressure
The pressures of intake and exhaust manifolds can be presented with the first law of thermodynamics and ideal gas law [13]. Intake manifold pressure is thus defined as

$$\dot{p}_i = \frac{R_i T_i}{V_i} \dot{m}_i \tag{3}$$

and exhaust manifold pressure is defined as

$$\dot{p}_x = \frac{R_x T_x}{V_x} \dot{m}_x \tag{4}$$

where, R $(J \cdot mol^{-1} \cdot K^{-1})$, T (K) and V (m^3) are the intake and exhaust manifold gas constant, temperature and volume respectively. By substituting (1) and (2) into (3) and (4) respectively, the pressure of intake and exhaust manifold become

$$\dot{p}_i = \frac{R_i T_i}{V_i} (W_{ci} - W_{ie}) \tag{5}$$

$$\dot{p}_x = \frac{R_x T_x}{V_x} (W_{ie} + W_f - W_{xt}) \tag{6}$$

Air flow through the cylinders can be presented as a function of engine speed, ω_e $(rad \cdot s^{-1})$, volumetric efficiency of the engine, η_v, and intake manifold pressure, p_i (Pa)

$$W_{ie} = \frac{\eta_v(\omega_e)\omega_e p_i V_d}{2\pi v R_i T_i} \tag{7}$$

where, V_d (m^3) is engine displacement volume and v is number of revolution per engine cycle. η_v is as defined in [14] as

$$\eta_v = a_{v1} + a_{v2}\omega_e + a_{v3}\omega_e^2$$

Values of constants a_{v1}, a_{v2} and a_{v3} are approximated.

The exhaust gas flow through the turbine can be presented with the orifice equation

$$W_{xt} = \frac{p_x}{\sqrt{R_x T_x}} A_t \Psi\left(\frac{p_a}{p_x}\right) f(u_{uvg}) \tag{8}$$

where, A_t (m^2) is the area of turbine nozzle and Ψ is the pressure ratio correction factor, which is defined as

$$\Psi\left(\frac{p_a}{p_x}\right) = \begin{cases} \sqrt{\frac{2\gamma}{\gamma-1}\left(\left(\frac{p_a}{p_x}\right)^{\frac{2}{\gamma}} - \left(\frac{p_a}{p_x}\right)^{\frac{\gamma+1}{\gamma}}\right)} & \text{, if } \frac{p_a}{p_x} > \left(\frac{2}{\gamma+1}\right)^{\frac{\gamma}{\gamma-1}} \\ \gamma^{\frac{1}{2}}\left(\frac{2}{\gamma+1}\right)^{\frac{\gamma+1}{2(\gamma-1)}} & \text{, if } \frac{p_a}{p_x} \le \left(\frac{2}{\gamma+1}\right)^{\frac{\gamma}{\gamma-1}} \end{cases}$$

Here, γ is specific heat ratio and it is defined as $\gamma = c_p/c_v$, where c_p $(J \cdot Kg^{-1}K^{-1})$ is specific heat at constant pressure and c_v $(J \cdot Kg^{-1}K^{-1})$ is specific heat at constant volume and p_a is ambient pressure. $f(u_{vgt})$ is the control signal and it is defined as

$$f(u_{vgt}) = b_1 + b_2 u + b_3 u^2 \tag{9}$$

where u_{vgt} is the control signal of variable geometry turbocharger (VGT), and b_1, b_2 and b_3 are approximated parameters [4]. Mass flow through the compressor is function the compressor isentropic efficiency η_c

$$W_{ci} = \frac{\eta_c P_c}{c_p T_a\left(\left(\frac{p_i}{p_a}\right)^{\mu} - 1\right)} \tag{10}$$

where T_a is ambient temperature and $\mu = (\gamma - 1)/\gamma$.

Power
Power of turbocharger is defined as power transferred between the turbine, P_t (kW), and compressor, P_c

$$\dot{P}_c = \frac{1}{\tau_c}(\eta_m P_t - P_c) \tag{11}$$

where, τ_c (s) is turbocharge time constant and η_m is the turbine mechanical efficiency. P_t is function of exhaust gas mass flow, ambient and exhaust pressures

$$P_t = \eta_t W_{xt} c_p T_x \left(1 - \left(\frac{p_i}{p_a}\right)^{\mu}\right) \tag{12}$$

where T_x presented as function of air-to-fuel ratio(λ)[14]

$$T_x = T_i + a_{t1}\lambda^{a_{t2}} + a_{t3} \tag{13}$$

Here, a_{t1-3} are tuning coefficients.

2.2 Fuel-path model

The mean acceleration of the crankshaft of the engine can be described with the second law of Newton

$$J\dot{\omega}_e = \Sigma M \tag{14}$$

where J $(Kg \cdot m^2)$ is the moment of inertia of the engine and ΣM is sum torques effecting the crankshaft. These torques are indicated engine torque, M_e (Nm), friction torque, M_f, and load torque, M_l.

The equation of indicated engine torque is modeled under the assumption that indicated thermal efficiency is depended on engine speed and air-to-fuel ratio, λ,

$$M_e = \frac{W_f Q_{hv}}{\omega_e}\eta_i(\omega_e, \lambda) \tag{15}$$

where Q_{hv} $(MJ \cdot kg^{-1})$ is lower heating value of the fuel, W_f is the fuel mass flow and $\eta_i = (a_1 + a_2\omega_e + a_3\omega_e^2)(1 - a_4\lambda^{a_5})$ [14]. W_f is used as a control signal.

Friction torque M_f is caused by phenomena such as friction of crankshaft bearings or resistance between the piston rings and cylinder wall and is proportional to the friction mean effective pressure, f_{mep} (Pa), [15]

$$M_f = \frac{f_{mep} V_d}{2\pi v} \tag{16}$$

where f_{mep} is defined as

$$f_{mep} = C_1 + 48\frac{N_e}{1000} + 0.4S_P^2$$

Here, C_1 (Pa) is a constant, N_e (RPM) is the engine speed and S_p $(m \cdot s^{-1})$ is the mean piston speed. The load torque can be defined as an external input. Thus, the mean acceleration of the crankshaft becomes

$$J\dot{\omega}_e = M_e - M_f - M_l \tag{17}$$

2.3 Linearization and analysis

A linearised model is needed to better understand the behavior of the model around operating points $(p_{i0}, p_{x0}, P_{c0}, \omega_{e0},\ f(u_{vgt0}))$. The mean value model of this work is linearised utilizing the Taylor's approximation. Detailed calculation have been left out for clarification.

Intake manifold pressure

$$\begin{aligned}\Delta\dot{p}_i = \frac{R_i T_i}{V_i}\Bigg[&\Bigg(-\frac{\eta_c P_{c0}\mu(\frac{p_{i0}}{p_a})^{\mu-1}(\frac{1}{p_a})}{c_p T_a((\frac{p_{i0}}{p_a})^{\mu}-1)^2} \\ &- \frac{\eta_v(\omega_{e0})\omega_{e0}V_d}{2\pi v R_i T_i}\Bigg)\Delta p_i \\ &+ \left(\frac{\eta_c}{c_p T_a((\frac{p_{i0}}{p_a})^{\mu}-1)}\right)\Delta P_c \\ &+ \left(\frac{p_{i0}V_d}{2\pi v R_i T_i}(a_{v1} + 2a_{v2}\omega_{e0} + 3a_{v3}\omega_{e0}^2)\right)\Delta\omega_e\Bigg]\end{aligned} \tag{18}$$

Exhaust manifold pressure

$$\begin{aligned}\Delta\dot{p}_x = \frac{R_x T_x}{V_x}\Bigg[&\left(-\frac{A_t\frac{d\Psi}{dp_{x0}}(\frac{p_a}{p_{x0}})}{\sqrt{R_x T_x}}f(u_{vgt0})\right)\Delta p_x \\ &+ \left(\frac{\eta_v(\omega_{e0})\omega_{e0}V_d}{2\pi v R_i T_i}\right)\Delta p_i \\ &+ \left(\frac{p_{i0}V_d}{2\pi v R_i T_i}(a_{v1} + 2a_{v2}\omega_{e0} + 3a_{v3}\omega_{e0}^2)\right)\Delta\omega_e \\ &+ \Delta W_f + \left(-\frac{p_{x0}A_t\Psi(\frac{p_a}{p_{x0}})}{\sqrt{R_x T_x}}\right)\Delta f(u_{vgt})\Bigg]\end{aligned} \tag{19}$$

Compressor power

$$\begin{aligned}\Delta\dot{P}_c = \frac{1}{\tau}\Bigg[&-\Delta P_c \\ &+ \left(\frac{\eta_m\eta_t A_t\frac{d\Psi}{dp_{x0}}(\frac{p_a}{p_{x0}})c_p T_x}{\sqrt{R_x T_x}}f(u_{vgt0})\right. \\ &\left.\left(\mu(\frac{p_a}{p_{x0}}^{\mu}) + (1 - (\frac{p_a}{p_{x0}})^{\mu})\right)\right)\Delta p_x \\ &+ \eta_m\eta_t\frac{p_{x0}A_t\Psi(\frac{p_a}{p_{x0}})}{\sqrt{R_x T_x}}c_p T_x\left(1 - (\frac{p_a}{p_{x0}})^{\mu}\right)\Delta f(u_{vgt})\Bigg]\end{aligned} \tag{20}$$

Engine speed

$$\Delta\dot{\omega}_e = \frac{1}{J}\Bigg[\Bigg(\frac{(a_2 + 2a_3\omega_{e0})(1 - a_4\lambda^{a_5})\omega_{e0}W_{f0}Q_{hv}}{\omega_{e0}^2} - \frac{(a_1 + a_2\omega_{e0} + a_3\omega_{e0}^2)(1 - a_4\lambda^{a_5})W_{f0}Q_{hv}}{\omega_{e0}^2}\Bigg)\Delta\omega_e + \Bigg(\frac{(a_1 + a_2\omega_{e0} + a_3\omega_{e0}^2)(1 - a_4\lambda^{a_5})Q_{hv}}{\omega_{e0}}\Delta W_f\Bigg) + \Delta load\Bigg] \quad (21)$$

With (18)-(21), the state-state representation of the linearised MIMO-system (Multiple Input, Multiple Output) becomes

$$\begin{aligned}\dot{x}(t) &= A\mathbf{x}(t)_{4\times1} + B\mathbf{u}(t)_{2\times1} + E\mathbf{d}(t)_{1\times1}\\ y(t) &= C\mathbf{x}(t)_{4\times1} + D\mathbf{u}(t)_{2\times1}\end{aligned} \quad (22)$$

where $A \in \mathbb{R}^{4\times4}$, $B \in \mathbb{R}^{4\times2}$. $E \in \mathbb{R}^{4\times1}$, $C \in \mathbb{R}^{2\times4}$ and $D \in \mathbb{R}^{2\times2}$. E is external disturbance, which in the case of this systems is the engine load torque.

3 Control design

Before designing a proper controller, two-way interaction of the MIMO-system has be to analyzed. Ideal case is to have as minimal internal coupling as possible. Such features of the system can be examined with the relative gain array (RGA) method [16]

$$RGA(G(s)) = \Lambda(G(s)) \triangleq G(s) \times (G(s)^{-1})^T \quad (23)$$

where $G(s)$ is the transfer function matrix of the system and $\times$ is the Hadamard product (point-by-point product). In this work the transfer function of the system is

$$G(s) = \begin{bmatrix} G_{11}(s) & G_{12}(s) \\ G_{21}(s) & G_{22}(s)\end{bmatrix}, \Lambda(G(s)) = \begin{bmatrix}\varepsilon & 1 \\ 1 & 0\end{bmatrix} \quad (24)$$

Although the engine speed is one of the inputs for intake manifold pressure as shown in (18), there is only a minor coupling between the channels. Value of ε is close to zero. The Λ-matrix is anti-diagonal due to order of the states, when defining the transfer function.

The results of RGA-analysis enable the separate control design of pressure and engine speed. In this work a separate PID-controller was utilized for each physical quantity in both nonlinear and linear model. The controller outputs are fuel injection and control of variable geometry turbocharger u_{vgt}. Similar results in both nonlinear and linear model mean that advanced control systems can be applied on the linearised system.

4 Simulation results

4.1 Nonlinear and linear open-looped system

The open-loop airpath and fuel-path models were initially simulated without controllers using step functions for inputs W_f and u with MATLAB's Simulink. According to the RGA-analysis, there is little coupling between the engine speed and intake manifold pressure. This can be seen in Figures 2 and 3, where increase of u at time 200 ms does not have any effect on the engine speed, and increase of W_f at 400 ms can be seen as a small peak in pressure curve. Major changes in the curves are caused by increase of engine load at 600 ms. All models

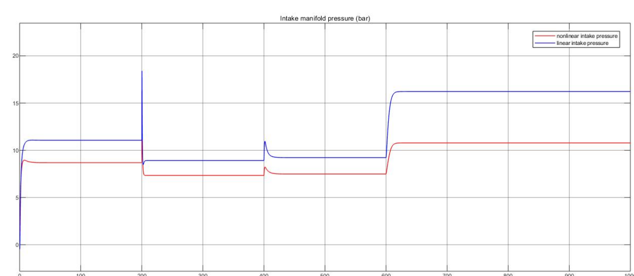

Fig. 2. Nonlinear (red) and linear (blue) intake manifold pressure of an open-looped system.

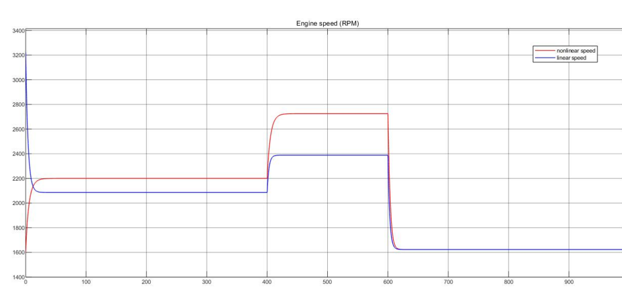

Fig. 3. Nonlinear (red) and linear (blue) engine speed of an open-loop system.

are Lyapunov stable as well as BIBO-stable (Bounded Input, Bounded Output). The deviation between the final values of nonlinear and linear pressure curves means that the models have different operating points.

4.2 Nonlinear controlled system

Simulation results of the nonlinear airpath and engine speed model are depicted in Figures 4 and 5. Both models are controlled with separate PID-controllers, where the input signals are W_f and u_{vgt} for airpath and engine speed model respectively. Intake manifold pressure

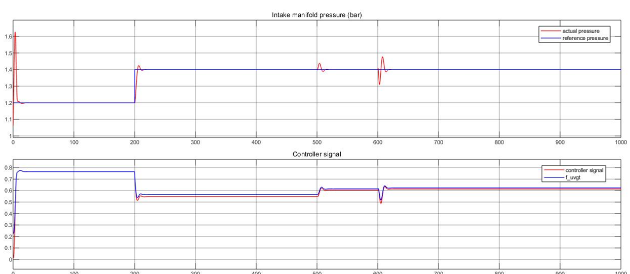

Fig. 4. Nonlinear intake manifold pressure (red) with respect to controller signal.

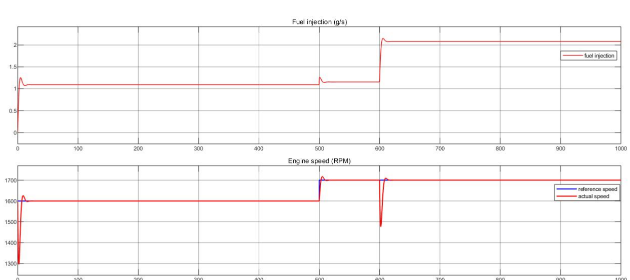

Fig. 5. Nonlinear engine speed (red) with respect to fuel injection.

is inversely proportional to the control signal as shown in Figure 4 at 200 ms. Increase of speed and external engine load can be seen as small peaks at 500 ms and 600 ms respectively. The increase of intake manifold pressure does not affect the engine speed. Increase of load causes the speed to drop, which is stabilized by fuel injection. Both models maintain the desired values despite the changes and disturbances affecting the system.

4.3 Linear controlled system

Simulation results of linearised, closed-loop intake manifold pressure and engine speed system are presented in Figures 6 and 7 respectively. As observed in section

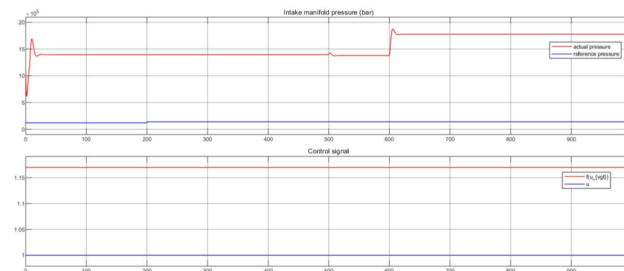

Fig. 6. Linear intake manifold pressure with respect to controller signal.

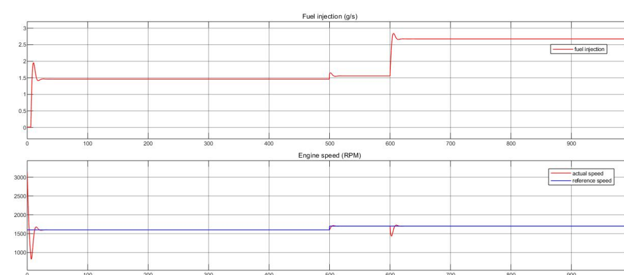

Fig. 7. Linear engine speed with respect to fuel injection.

4.1, the airpath model is strongly dependent on operating points. The controller signal is at its peak during the entire simulation time and for this reason the pressure does not drop to its reference value. This means that the linear airpath model has different operating point than the nonlinear model. Engine speed is stabilized within a short time and follows the reference value well, which is seen as overlapping curves in Figure 7. Major difference to the nonlinear engine speed model is a slight increase of fuel injection at 600 ms.

5 Conclusions

The purpose of this work was to design a first principles mean value model for the airpath and fuel-path of a maritime diesel engine to reduce fuel consumption and thus, increase the efficiency. To achieve this, a nonlinear and linearised model were simulated with PID-controllers.

Initially, simulations were performed without any controllers and the results indicated that the outcome of airpath model depended heavily on the operating points. This problem occurred again in the closed-loop simulations. Nonlinear models provided sufficient results. However, advanced control approaches cannot be performed on nonlinear systems.

Proper operating points can be found with methods, such as pole placement or numerical approximation. This is a challenging problem due to complexity of the simulated systems. Only then, the model can be further developed with other control algorithms and utilized for more accurate models used for cylinder-wise control the diesel engines.

It will be left as an open question, how this situation should be observed and the problem removed.

6 Acknowledgement

In doing this work the co-operation with Wärtsilä Oyj Apb is greatly appreciated.

References

[1] European Commission. Emission in the automotive sector. URL https://ec.europa.eu/growth/sectors/automotive/environment-protection/emissions_en.

[2] International Maritime Organization. Nitrogen oxides (nox) - regulation 13. URL http://www.imo.org/en/OurWork/Environment/PollutionPrevention/AirPollution/Pages/Nitrogen-oxides-(NOx)-%E2%80%93-Regulation-13.aspx.

[3] J. Aalto-Setälä. Adaptive wastegate control of combustion engines, 2013.

[4] S. Samokhin. *Adaptive control of conventional and hybrid marine diesel engines subject to uncertain or time-varying dynamics*. Phd thesis, Aalto University, 2018.

[5] A. G. Stefanopoulou, I. Kolmanovsky, and J. S. Freudenberg. Control of variable geometry turbocharged diesel engines for reduced emissions. In *Proceedings of the 1998 American Control Conference. ACC (IEEE Cat. No.98CH36207)*, volume 3, pages 1383–1388 vol.3, June 1998. 10.1109/ACC.1998.707043.

[6] M. Jankovic and I. Kolmanovsky. Robust nonlinear controller for turbocharged diesel engines. In *Proceedings of the 1998 American Control Conference. ACC (IEEE Cat. No.98CH36207)*, volume 3, pages 1389–1394 vol.3, June 1998. 10.1109/ACC.1998.707047.

[7] M. Jung and K. Glover. Calibratable linear parameter-varying control of a turbocharged diesel engine. *IEEE Transactions on Control Systems Technology*, 14(1):45–62, Jan 2006. ISSN 1063-6536. 10.1109/TCST.2005.860513.

[8] A. Plianos and R. Stobart. Dynamic feedback linearization of diesel engines with intake variable valve actuation. In *2007 IEEE International Conference on Control Applications*, pages 455–460, Oct 2007. 10.1109/CCA.2007.4389273.

[9] L. Kocher, E. Koeberlein, K. Stricker, D. G. Van Alstine, B. Biller, and G. M. Shaver. Control-oriented modeling of diesel engine gas exchange. In *Proceedings of the 2011 American Control Conference*, pages 1555–1560, June 2011. 10.1109/ACC.2011.5991425.

[10] Gabriel Turesson. *Model-Based Optimization of Combustion-Engine Control*. PhD thesis, Lund University, 06 2018.

[11] Vebic's engine laboratory starts operating. URL https://www.univaasa.fi/en/news/vebicin_moottorilaboratorio_kaynnistyi/.

[12] L. Guzzella and C.H. Onder. *Introduction to Modeling and Control of Internal Combustion Engine Systems*. Number 2nd ed. Springer-Verlag Berlin Heidelberg, 2010. ISBN 978-3-642-10775-7.

[13] Johan Wahlström and Lars Eriksson. Modeling of a diesel engine with vgt and egr capturing sign reversal and non-minimum phase behaviors. Technical Report 2882, Linköping University, Vehicular Systems, 2009. URL http://urn.kb.se/resolve?urn=urn:nbn:se:liu:diva-18484.

[14] L. Guzzella and A. Amstutz. Control of diesel engines. *IEEE Control Systems Magazine*, 18(5):53–71, Oct 1998. ISSN 1066-033X. 10.1109/37.722253.

[15] J.B. Heywood. *Internal Combustion Engine Fundamentals*. Automotive technology series. McGraw-Hill, 1988. ISBN 9780071004992. URL https://books.google.fi/books?id=O69nQgAACAAJ.

[16] Sigurd Skogestad and Ian Postlethwaite. *Multivariable Feedback Control: Analysis and Design*. John Wiley & Sons, Inc., USA, 2005. ISBN 0470011688.